

Detection of $\text{Ly}\beta$ auto-correlations and $\text{Ly}\alpha$ - $\text{Ly}\beta$ cross-correlations in BOSS Data Release 9

Vid Iršič,^a Anže Slosar,^b Stephen Bailey,^c Daniel J. Eisenstein,^d Andreu Font-Ribera,^{e,c} Jean-Marc Le Goff,^f Britt Lundgren,^g Patrick McDonald,^c Ross O’Connell,^h Nathalie Palanque-Delabrouille,^f Patrick Petitjean,ⁱ Jim Rich,^f Graziano Rossi,^f Donald P. Schneider,^{j,k} Erin S. Sheldon^b Christophe Yèche^f

^aFaculty of Mathematics and Physics, University of Ljubljana, Jadranska 19, 1000 Ljubljana, Slovenia

^bBrookhaven National Laboratory, Blgd 510, Upton NY 11375, USA

^cLawrence Berkeley National Laboratory, 1 Cyclotron Road, Berkeley, CA 94720, USA

^dHarvard-Smithsonian Center for Astrophysics, MS #20, 60 Garden St., Cambridge, MA 02138, USA

^eInstitute of Theoretical Physics, University of Zurich, Winterthurerstrasse 190, 8057 Zurich, Switzerland

^fCEA, Centre de Saclay, IRFU, F-91191 Gif-sur-Yvette, France

^gDepartment of Astronomy, University of Wisconsin, 475 North Charter Street, Madison, WI 53706, USA

^hPhysics Department, Carnegie Mellon University, Pittsburgh, PA 15213, USA

ⁱUniversité Paris 6 et CNRS, UMP7095, Institut d’Astrophysique de Paris, 98bis Boulevard Arago, 75014 Paris, France

^jDepartment of Astronomy and Astrophysics, The Pennsylvania State University, University Park, PA 16802, USA

^kInstitute for Gravitation and the Cosmos, The Pennsylvania State University, University Park, PA 16802, USA

E-mail: vid.irsic@fmf.uni-lj.si, anze@bnl.gov

Abstract. The Lyman- β forest refers to a region in the spectra of distant quasars that lies between the rest-frame Lyman- β and Lyman- γ emissions. The forest in this region is dominated by a combination of absorption due to resonant Ly α and Ly β scattering. When considering the 1D Ly β forest in addition to the 1D Ly α forest, the full statistical description of the data requires four 1D power spectra: Ly α and Ly β auto-power spectra and the Ly α -Ly β real and imaginary cross-power spectra. We describe how these can be measured using an optimal quadratic estimator that naturally disentangles Ly α and Ly β contributions. Using a sample of approximately 60,000 quasar sight-lines from the BOSS Data Release 9, we make the measurement of the one-dimensional power spectrum of fluctuations due to the Ly β resonant scattering. While we have not corrected our measurements for resolution damping of the power and other systematic effects carefully enough to use them for cosmological constraints, we can robustly conclude the following: i) Ly β power spectrum and Ly α -Ly β cross spectra are detected with high statistical significance; ii) the cross-correlation coefficient is ≈ 1 on large scales; iii) the Ly β measurements are contaminated by the associated OVI absorption, which is analogous to the SiIII contamination of the Ly α forest. Measurements of the Ly β forest will allow extension of the usable path-length for the Ly α measurements while allowing a better understanding of the physics of intergalactic medium and thus more robust cosmological constraints.

Keywords: cosmology, Ly β forest, Ly α forest, large scale structure

Contents

1	Introduction	1
2	Description of the $\text{Ly}\alpha$ and $\text{Ly}\beta$ forests	3
2.1	Power spectra of fluctuations	3
2.2	Theoretical expectation for $P_{\beta\beta}$, $P_{\alpha\beta}$ and $Q_{\alpha\beta}$	4
2.3	Measuring power spectra from the data	5
2.4	Metal contamination at small velocity separations	10
3	Data & Synthetic data	11
3.1	Mock data	12
4	Application to mock data	12
5	Results	14
6	Conclusion	17

1 Introduction

Lyman- α forest is a series of absorption lines, blue-ward of the $\text{Ly}\alpha$ emission in the spectra of high-redshift quasars. Although it was discovered nearly half a century ago [23], it only recently became a useful cosmological probe [39, 40]. An important part in this evolution was due to the technological progress that made it possible for large surveys such as Sloan Digital Sky Survey (SDSS, [1, 2, 4–6, 10, 12, 13, 16, 18, 20–22, 29, 31, 33, 36, 41]) to measure spectra of quasars reliably and in large numbers.

The physical picture of the $\text{Ly}\alpha$ forest was established in the 1990s. The absorption features primarily arise in the near-mean density regions [3, 7, 42] from the weakly non-linear fluctuations of gas held in equilibrium by photo-ionizing background radiation [19, 38]. This makes it possible for the $\text{Ly}\alpha$ forest fluctuations to be predicted from first principles using large numerical simulations. Namely, the complicated astrophysics of fluid dynamics, baryon-condensation, star-formation and feedback due to supernova and active galactic nuclei activity is absent - a typical line of sight does not pierce through a virialized object, and when it does, it results in a complete absorption, which makes detailed modeling of dense regions inessential. While this makes predictions of $\text{Ly}\alpha$ quantities considerably easier than galaxy evolution, the physics of intergalactic medium (IGM) remains complicated and any results must be cross-checked in as many different ways as possible.

The field has settled on using the one-dimensional power spectrum $P_F(k, z)$ of the relative fluctuations in the transmitted flux fraction δ_F as the quantity of choice when comparing observations with the theoretical predictions [8, 9, 25, 26, 28]. The main reason for this selection is that the power spectrum of transmitted flux fluctuations is observationally closest to the data: it is essentially an appropriately scaled version of the actual fluctuations in the observed forest and hence it is easy to understand the systematics and the noise properties of the measurement. Choosing the power spectrum over the correlation function more cleanly decouples the scales involved. For example, fluctuations due to poor understanding of the continuum are restricted to large scales.

Recently, the three-dimensional correlations have been measured in the Ly α forest ([6, 34, 35]) and it may eventually be possible to make a unified analysis of both 1D and 3D correlations. However, systematic issues are very different in the two cases and at present the 1D power spectrum of fluctuations is our best approach for measuring the linear power spectrum amplitude at scales around $k \sim 1h/\text{Mpc}$.

As discussed above, systematic control of astrophysical and instrumental effects remains one of the largest challenges in the Ly α studies. There are two main ways to independently measure the properties of the IGM and thus cross-check the assumptions. The first one is to use a higher order statistic (bispectrum or trispectrum, [17, 24, 28]). This approach allows one to measure essentially the same quantities as in the power spectrum with a similar signal-to-noise, but with largely independent or differently-scaling systematics. An alternative is to use higher order Lyman absorption, which was proposed in [11] and which we study in this work.

Understanding the Ly β forest would be useful in several ways. First and foremost, the Ly β forest probes the same hydrogen gas, but with a smaller optical depth at a given column density of gas. Fortunately, there is no uncertainty in the ratio of optical depths, since it is entirely determined by atomic physics. The ratio of cross sections for Lyman series lines simplifies to the ratio of oscillator strength for those lines, which can be calculated analytically. The oscillator strength of Lyman transition of order n is given by ([32])

$$f_n = 2^8 n^5 \frac{(n-1)^{2n-4}}{3(n+1)^{2n+4}}. \quad (1.1)$$

The ratio of the optical depths for β and α lines $r_{\beta\alpha}$ is thus given by

$$r_{\beta\alpha} = \frac{\tau_\beta}{\tau_\alpha} = \frac{f_3}{f_2} \approx 0.1901. \quad (1.2)$$

Therefore, the Ly β can better probe regions of higher density. When used in conjunction with the Ly α absorption, it can break degeneracies in the modeling of these regions.

At the same time, the absorption in the Ly β region of the forest is dominated by the Ly α absorption. Therefore, if one is able to simultaneously model the Ly α and Ly β regions, it is possible to extend the useful path length for Ly α forest by up to 20% (depending on the redshift distribution of quasars in a given survey). This can, for example, significantly increase the sensitivity to the baryon acoustic oscillations signal, without any increase in the cost of an experiment.

The purpose of this paper is to make a proof-of-concept measurement of the Ly β forest in the DR9 data release of Baryon Oscillation Spectroscopic Survey (BOSS; [4, 10]), which is part of the Sloan Digital Sky Survey III collaboration ([12, 16, 18, 20, 36, 41]). We believe our detection significance is robust and the results are correct and consistent with expectations. However, these measurements should not be used to constrain cosmological parameters: our understanding of the resolution uncertainty, noise bias and other subtleties is limited. Moreover, the results are strong enough to show that these measurements are clearly feasible with high precision. For example, even with our limited understanding of systematics, we are able to measure a contaminating metal line in the Ly β forest with percent level accuracy on its wavelength and identify it as the OVI feature.

The paper is structured as follows. In Section 2 we present the theoretical description of the fluctuations and how physically relevant quantities can be derived from the data. The

data and simulations used are discussed on in Section 3. In Section 4 we present the results on the mock data and in Section 5 we show the final measurements on the data. We conclude in Section 6.

2 Description of the Ly α and Ly β forests

2.1 Power spectra of fluctuations

The spectrum for a quasar q at an observed wavelength λ_o is given by

$$f^q(\lambda_o) = C^q(\lambda_r)F^q(\lambda_o), \quad (2.1)$$

where $C^q(\lambda_r)$ is the intrinsic quasar spectrum (observed by an observer in the rest frame of the quasar with redshift z_q , where $\lambda_r = \lambda_o/(1 + z_q)$) and $F(\lambda_o)$ is the total absorption due to absorbing material along the line of sight to the quasars

$$F^q(\lambda_o) = \prod_{i, (z_i < z_q)} e^{-\tau_i^q(r=c \ln \lambda_o/\lambda_i)}, \quad (2.2)$$

where τ_i is the optical depth for the i -th component absorbing at rest-frame λ_i and c is speed of light. Optical depth is a function of distance, which we parametrise in terms of the logarithm of the observed wavelength. The reason for this choice is that the difference in this distance measure is expressed in the usual units of kms^{-1} . The crucial point is that for a given observed-frame wavelength, we allow for several absorbers that occupy different positions along the line of sight to the quasar. Of course, since matter behind the quasar cannot absorb light, any given component can absorb only at sufficiently small observed wavelengths. In other words, Ly α absorption can be found blue-ward of the rest-frame Ly α emission, the Ly β absorption blue-ward of the rest-frame Ly β emission, etc.

In Ly α forest studies, it is usually assumed that the Ly α absorption is the dominant source of absorption and worked in terms of the relative transmitted flux fluctuations

$$F^q(\lambda_o) = e^{-\tau_\alpha^q} = \bar{F}_\alpha(r^\alpha)(1 + \delta_\alpha^q(r^\alpha)), \quad (2.3)$$

where $r^\alpha = c \ln \lambda_o/\lambda_\alpha$ is our radial coordinate. We therefore describe the fluctuations in the forest as relative fluctuations around the mean absorption. The mean of those fluctuations is $\langle \delta^q \rangle = 0$ and the two point function is conveniently described in terms of the correlation function $\xi_{\alpha\alpha}(x, z)$

$$\langle \delta_\alpha(r_1^\alpha) \delta_\alpha(r_2^\alpha) \rangle = \xi_{\alpha\alpha}(x = r_2^\alpha - r_1^\alpha = \ln \lambda_2/\lambda_1, \bar{z}). \quad (2.4)$$

or equivalently the power spectrum

$$\xi_{\alpha\alpha}(x, \bar{z}) \equiv \frac{1}{2\pi} \int_{-\infty}^{\infty} P_{\alpha\alpha}(k, \bar{z}) e^{-kx} dk = \frac{1}{\pi} \int_0^{\infty} P_{\alpha\alpha}(k, \bar{z}) \cos(kx) dk, \quad (2.5)$$

where \bar{z} is defined as

$$1 + \bar{z} = \frac{\sqrt{\lambda_1 \lambda_2}}{\lambda_\alpha}. \quad (2.6)$$

Here and henceforth in this paper λ_1 and λ_2 are observed wavelengths (λ_o) at two different positions in the quasar spectrum. They should not be confused by rest-frame wavelength

of absorbing material λ_i from Equation 2.2 which is, in this work, replaced by Ly α rest-frame absorption wavelength $\lambda_\alpha = 1215.67\text{\AA}$ and Ly β rest-frame absorption wavelength $\lambda_\beta = 1025.72\text{\AA}$.

The power spectrum in Equation 2.5 is consistent with standard definitions found elsewhere in the literature [8, 27, 37].

We proceed by adding the absorption by the Ly β line. In this case, where considering a pixel in the Ly β forest, we have

$$F^q(\lambda_o) = e^{-\tau_\alpha^q - \tau_\beta^q} = \bar{F}_\alpha(z_\alpha) \bar{F}_\beta(z_\beta) (1 + \delta_\alpha^q(r^\alpha)) (1 + \delta_\beta^q(r^\beta)) = \bar{F}_T(\lambda_o) (1 + \delta_T(\lambda_o)). \quad (2.7)$$

Any given pixel in the Ly β forest thus receives a contributions to the absorption from gas residing at two distinct redshifts. One can distinguish between the two components only statistically, by observing the total relative fluctuation δ_T and cross-correlating it with other fluctuations in the Ly α and Ly β forests (see section 2.3). The two-point function of the Ly β forest is given by Equations (2.4) and (2.5). The cross-power is slightly more subtle:

$$\left\langle \delta_\alpha(r_1^\alpha) \delta_\beta(r_2^\beta) \right\rangle = \xi_{\alpha\beta} \left(x = r_2^\beta - r_1^\alpha = \ln \left[\frac{(\lambda_2/\lambda_\beta)}{(\lambda_1/\lambda_\alpha)} \right], \bar{z}_{\alpha\beta} \right), \quad (2.8)$$

where $\bar{z}_{\alpha\beta}$ is defined as

$$1 + \bar{z}_{\alpha\beta} = 1 + \bar{z}_{\beta\alpha} = \sqrt{\frac{\lambda_1 \lambda_2}{\lambda_\alpha \lambda_\beta}} \quad (2.9)$$

It is evident from this definition that

$$\xi_{\alpha\beta}(x, \bar{z}_{\alpha\beta}) = \xi_{\beta\alpha}(-x, \bar{z}_{\alpha\beta}) \neq \xi_{\alpha\beta}(-x, \bar{z}_{\alpha\beta}), \quad (2.10)$$

since for absorption by two clouds of gas at mean redshift $\bar{z}_{\alpha\beta}$, the expectation value of the correlation is different for the case of a lower-redshift cloud absorbing in α and a higher redshift cloud absorbing in β or vice-versa. As a result, the correlation function is not symmetric around zero and the cross-power spectrum has both real and imaginary components:

$$\xi_{\alpha\beta}(x, \bar{r}) = \frac{1}{2\pi} \int_{-\infty}^{\infty} [P_{\alpha\beta}(k, \bar{z}) + iQ_{\alpha\beta}(k, \bar{z})] e^{-ikx} dk. \quad (2.11)$$

There exists no apriori argument that the imaginary part of the cross-power spectrum should be zero. Since a non-zero $Q_{\alpha\beta}$ reflects a non-symmetric problem it must be studied for each specific case separately. In the next subsection we elaborate why a non-zero $Q_{\alpha\beta}$ is expected in Ly α -Ly β correlations.

A complete statistical description of Ly α and Ly β fluctuations at the two-point level is thus given by four power spectra $P_{\alpha\alpha}$, $P_{\beta\beta}$, $P_{\alpha\beta}$, $Q_{\alpha\beta}$. Each of these is a function of scale and redshift.

2.2 Theoretical expectation for $P_{\beta\beta}$, $P_{\alpha\beta}$ and $Q_{\alpha\beta}$

Before proceeding, let us briefly discuss the expected quantities to be measured by the new power spectra.

First, the reader might be confused as to whether the new quantities are truly linearly independent, since in the introduction we have argued that the ratio of the optical depths is deterministic and known from atomic physics. Indeed, they are independent for the following

reasons. Fluctuations in the optical depth are related to the fluctuations in the transmitted flux fraction via a non-linear transformation

$$\bar{F}(1 + \delta_F) = e^{-\bar{\tau}(1+\delta_\tau)} = e^{-\bar{\tau}}(1 - \bar{\tau}\delta_\tau + \frac{1}{2}\bar{\tau}^2\delta_\tau^2 \dots). \quad (2.12)$$

We immediately see that $\bar{F} \neq e^{-\bar{\tau}}$, since even zero-lag correlators contribute to the mean. Therefore, while $\bar{\tau}_\beta = r_{\beta\alpha}\bar{\tau}_\alpha$, it is not possible to write a similar relation between \bar{F}_α and \bar{F}_β . By the same token, any 2-point statistics in δ_F will contain contributions not just from the 2-point statistics of δ_τ , but also all higher-order correlators and hence one cannot write relations between $P_{\alpha\alpha}$ and, for example, $P_{\beta\beta}$.

We do know, however, that on very large scales in three-dimensions, both absorptions become linear tracers of the underlying density field. Consequently one expects the 3D cross-correlation coefficient to be close to unity

$$r_{3D}(k) = \frac{P_{3D\ \alpha\beta}(k)}{\sqrt{P_{3D\ \alpha\alpha}(k)P_{3D\ \beta\beta}(k)}} \sim 1 \text{ for small } k. \quad (2.13)$$

Of course, due to stochasticity in the biasing relation (taking form of white noise in the low k limit), the cross-correlation coefficient will be somewhat less than unity, but this effect is expected to be small (the absorption is, after all, coming from exactly the same structure along each line of sight).

More importantly, however, the 1D power spectrum aliases small-scale three-dimensional modes into large scale one-dimensional modes

$$P_{1D}(k) = \frac{1}{2\pi} \int_k^\infty P_{3D}(k')k'dk'. \quad (2.14)$$

Therefore the cross-correlation coefficient between Ly α and Ly β 1D power spectra, defined as

$$r = \left[\frac{P_{\alpha\beta}^2(k) + Q_{\alpha\beta}^2(k)}{P_{\alpha\alpha}(k)P_{\beta\beta}(k)} \right]^{1/2}, \quad (2.15)$$

is expected to be somewhat smaller than unity, but one would not expect $r \ll 1$ at small k .

Finally, in a non-evolving universe, $Q_{\alpha\beta} = 0$. The real Universe is evolving, but sufficiently slowly so that for small separations the approximation of stationary statistics is in general accurate. Hence, we expect $Q_{\alpha\beta}$ to be smaller than $P_{\alpha\beta}$, i.e., the cross-power spectrum to be approximately real. However, $Q_{\alpha\beta}$ is required for a statistically consistent complete description of fluctuations in a given spectrum and thus it should be measured together with other quantities.

2.3 Measuring power spectra from the data

We proceed by discussing the reconstruction of these power spectra from the data. The $P_{\alpha\alpha}$ can be extracted relatively directly, but other components are more difficult, because β absorption is always contaminated by the lower redshift α absorption.

The model that we use for the observed quasar spectrum is given by:

$$f^q(\lambda_i) = A^q \bar{C}(\lambda_i^{rest}) \bar{F}_T(z_i) (1 + \delta_T(\lambda_i)). \quad (2.16)$$

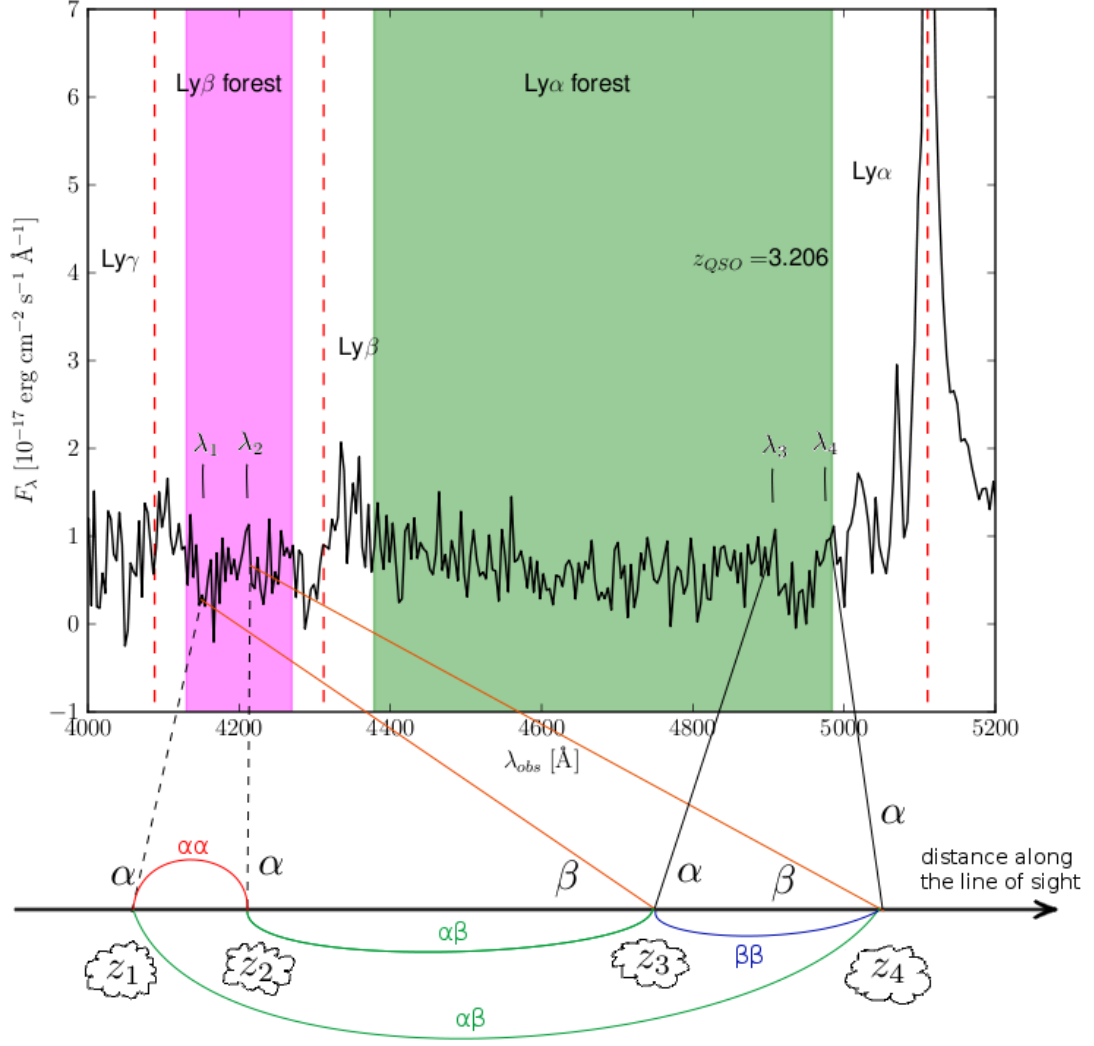


Figure 1. Geometry of the absorption in the α and β forests. A “cloud” of gas absorbing at redshift z_3 in Ly α is also absorbing in the Ly β forest. However, the same pixel in the Ly β forest is also subject to absorption by another “cloud” at redshift z_1 . Ditto for clouds at z_4 and z_2 . When cross-correlating two pixels residing in the β region of the quasar spectrum, one must take into account four contributions to the correlations. When cross-correlating a pixel in the Ly β forest with one in the Ly α forest, one must take into account two correlations.

The continuum in each quasar $C^q(\lambda_r)$ is modeled by a quasar amplitude A^q and the mean continuum $\bar{C}(\lambda_i^{rest})$. The absorption field is decomposed into a mean absorption

$$\bar{F}_T = \begin{cases} \lambda_r > \lambda_\alpha & 1 \\ \lambda_\alpha > \lambda_r > \lambda_\beta & F_\alpha(z) \\ \lambda_\beta > \lambda_r & F_\alpha(z)F_\beta(z) \end{cases} \quad (2.17)$$

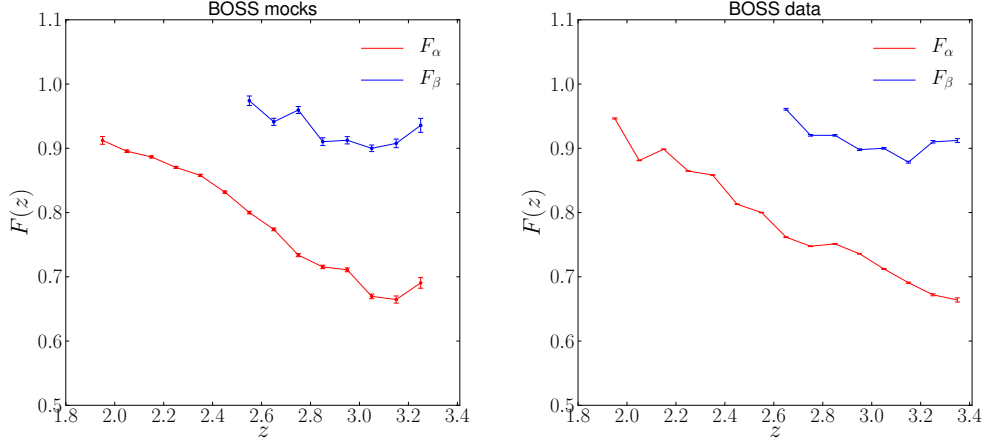


Figure 2. Mean flux of the Ly α and Ly β fields inferred from the mock data set (left) and from the real data (right). The error bars on both plots are underestimated since they assume independent forest pixels.

and fluctuations

$$1 + \delta_T = \begin{cases} \lambda_r > \lambda_\alpha & 1 \\ \lambda_\alpha > \lambda_r > \lambda_\beta & 1 + \delta_\alpha \\ \lambda_\beta > \lambda_r & (1 + \delta_\alpha)(1 + \delta_\beta). \end{cases} \quad (2.18)$$

In this work, we ignore the second order contributions in the Ly β forest

$$\delta_T(\lambda_o) = \delta_\alpha(r_\alpha) + \delta_\beta(r_\beta) + \delta_\alpha(r_\alpha)\delta_\beta(r_\beta) = \delta_\alpha(r_\alpha) + \delta'_\beta(r_\beta) \quad (2.19)$$

and thus work with effective fluctuations in the β forest

$$\delta'_\beta(r_\beta) = \delta_\beta(r_\beta) + \delta_\beta(r_\beta)\delta_\alpha(r_\alpha). \quad (2.20)$$

Note that while quadratic term cannot be neglected, because it is not small, it is for all practical purposes uncorrelated with the β forest as it corresponds to gas that is ~ 400 Mpc/h away – on scales considerably larger than the largest scales on which we measure the power spectrum. Under this approximation the second term in the above equation averages to zero. The cross correlation $\langle \delta'_\beta \delta_\alpha \rangle \sim \langle \delta_\beta \delta_\alpha \rangle = \xi_{\alpha\beta}$, but the auto-correlation gains an additional “noise” term $\langle \delta'_\beta \delta'_\beta \rangle \sim \xi_{\beta\beta} + \xi_{\beta\beta}\xi_{\alpha\alpha}$. The α auto-correlation is evaluated at the same distance separation $r = \Delta \log \lambda$, but at a lower redshift z_α

$$1 + z_\alpha = \frac{\lambda_\beta}{\lambda_\alpha} (1 + z). \quad (2.21)$$

Using the definition of the Fourier transform between correlation function the power spectrum from Equation (2.5) the corrected power spectrum can be written as

$$P'_{\beta\beta}(k, z) = P_{\beta\beta}(k, z) + \frac{1}{2\pi} P_{\beta\beta}(k, z) * P_{\alpha\alpha}(k, z_\alpha) = P_{\beta\beta}(k, z) + \frac{1}{2\pi} \int_{-\infty}^{\infty} P_{\beta\beta}(y, z) P_{\alpha\alpha}(k-y, z_\alpha) dy, \quad (2.22)$$

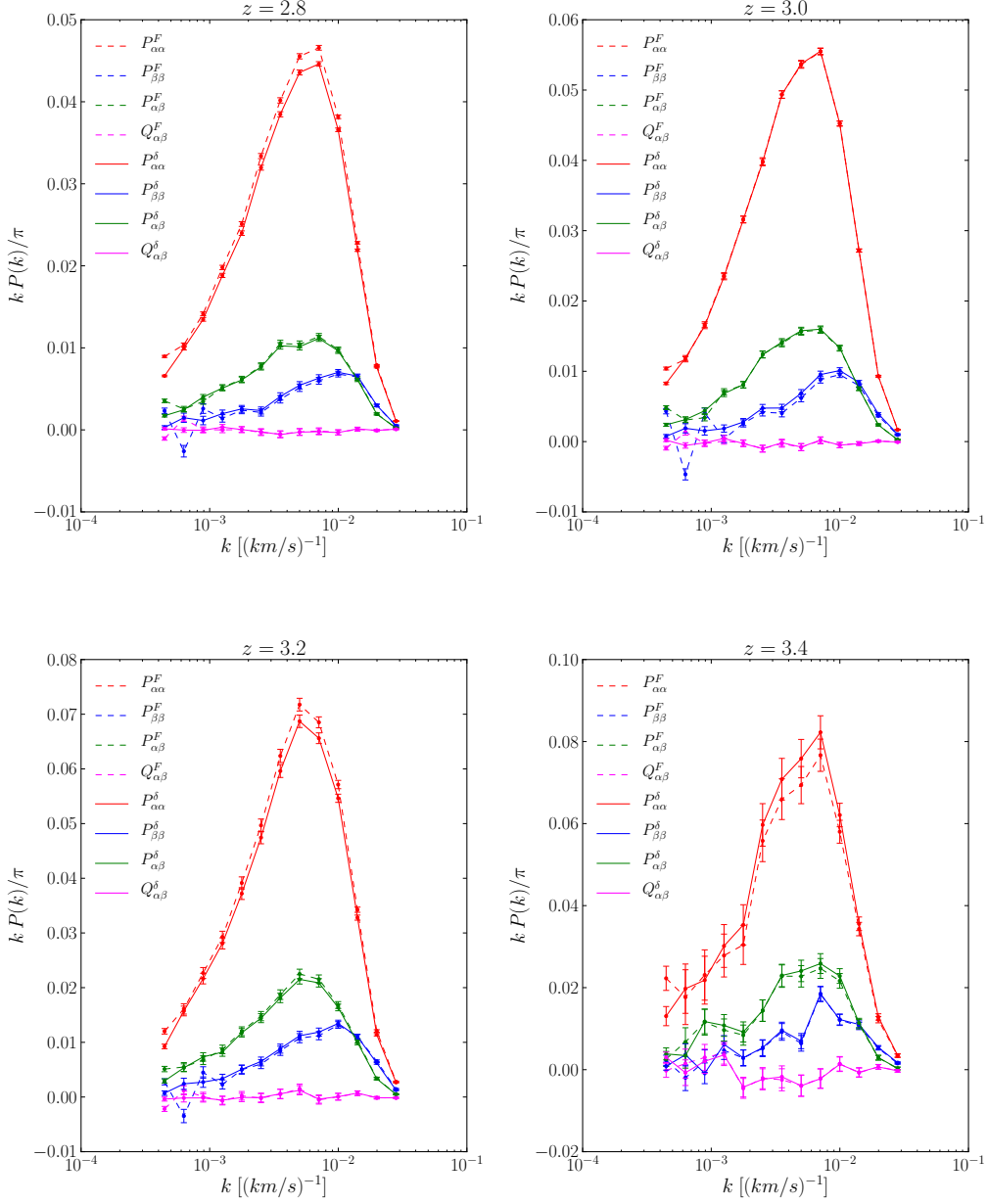


Figure 3. Power spectrum components measured on two different mock data sets: results with known quasar continua (solid line) and the full analysis (dashed line). This plot displays the mean of 10 realizations of 10000 QSO mock data set. No PSF deconvolution has been performed and hence the power drops to zero at large k values.

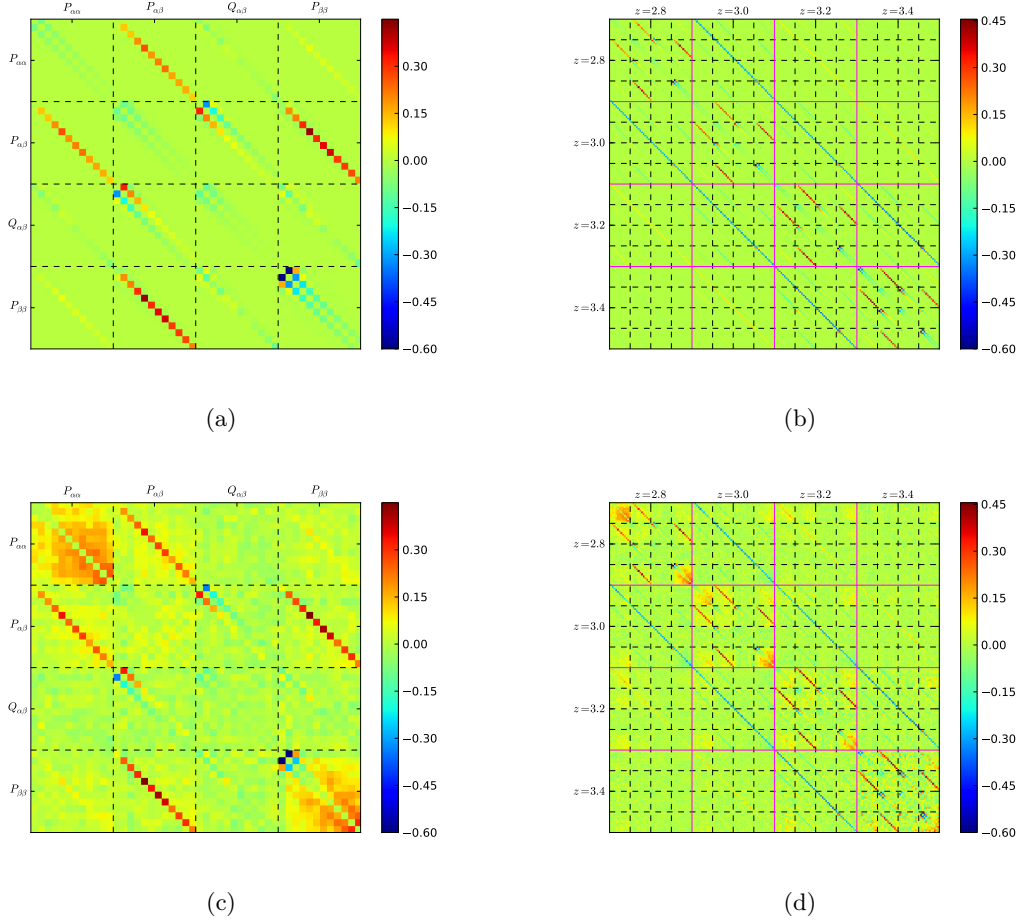


Figure 4. Error correlation matrices $\mathcal{C}_{ij} = C_{ij}/\sqrt{C_{ii}C_{jj}}$. Top row figures (a and b) are for estimator covariance matrix, while bottom row are for the bootstrap derived covariance matrix. The left side figures (a and c) are an expanded view of the sub-matrix at redshift $z = 2.8$ (upper left corner of the full matrix), while the right figures are the full matrices. The diagonal elements (unity) by definition were set to zero to increase the contrast. See text for discussion.

where $(*)$ stands for convolution. Assuming $P_{\alpha\alpha}$ and $P_{\beta\beta}$ to be approximately white, i.e., $P_{\alpha\alpha}(k, z) = \sigma_\alpha^2(z)$, where σ^2 is the variance of the field, the correction to the cross correlation coefficient is

$$r'_{\alpha\beta}(k, z) = r_{\alpha\beta}(k, z) \frac{1}{\sqrt{1 + \sigma_\alpha^2(z_\alpha)}} \approx r_{\alpha\beta}(k, z) \left(1 - \frac{\sigma_\alpha^2(z_\alpha)}{2}\right). \quad (2.23)$$

Since z_α is always smaller than z , for our highest measured redshift bin of $z = 3.4$, the corresponding z_α would be $z_\alpha = 2.74$. The variance at $z_\alpha = 2.74$ is approximately $\sigma_\alpha^2(2.74) = 0.08$ ([34, 35]) and since the variance is increasing with redshift ([34, 35]) this is the largest correction we would be able to apply. Thus, since the correction to the cross-correlation coefficient is less than 5%, the effect is well below what we can currently measure. It is important to note, however, that this will need to be carefully modeled for the future precision observations.

Under these approximations, we now drop a prime on δ_β and proceed with writing correlations between measured pixels in the spectrum. A correlation of one pixel in the Ly β forest with a pixel in the Ly α forest is given by

$$\langle \delta_\alpha(\lambda_1) \delta_T(\lambda_2) \rangle = \xi_{\alpha\alpha}(r_2^\alpha - r_1^\alpha) + \xi_{\alpha\beta}(r_2^\beta - r_1^\alpha) \quad (2.24)$$

and a correlation of two pixels in the Ly β forest contains four terms

$$\langle \delta_T(\lambda_1) \delta_T(\lambda_2) \rangle = \xi_{\alpha\alpha}(r_2^\alpha - r_1^\alpha) + \xi_{\beta\beta}(r_2^\beta - r_1^\beta) + \xi_{\alpha\beta}(r_2^\beta - r_1^\alpha) + \xi_{\alpha\beta}(-(r_1^\beta - r_2^\alpha)). \quad (2.25)$$

This is illustrated schematically in the Figure 1.

In this study we work within an optimal quadratic estimator framework using the same methodology (and code-base) as in [35]. In particular, we model the power spectrum functions P and Q as flat power-bands measured in 20 bins, from $k = 0.000445881$ to $k = 0.05$ in steps of $\log k = 0.1$. The lowest k bin was extended to $k = 0$. In redshift-direction, we use uniformly-spaced redshift bins from $z = 1.9$ to $z = 3.5$ in steps of 0.2 and the model interpolates between values determined at those redshifts. For Ly β and the cross power spectrum we use redshift bins from $z = 2.5$ to $z = 3.5$. The redshift corresponds to the true gas redshift, so Ly β absorption from a clump of gas at $z < 2.5$ is shifted into UV and thus not recorded by the SDSS-III data. There is little signal in lowest and highest redshift bins, but due to interpolation, we can recover some information.

In this parametrisation, the Ly β forest receives linear contributions from all power spectrum bins. Even in the case of the usual Ly α forest alone, however, a pair of pixels receives contributions from all power spectrum bins, and hence from the point of view of a quadratic estimator, our situation is not very different from the standard case.

In short, the basic data-analysis proceeds as follows:

- We start by measuring the mean continuum and absorption as described in [35]. This process has been extended to allow for an additional mean absorption in the β forest \bar{F}_β , but is otherwise the same as [35].
- We then measure only Ly α forest power spectrum using the mean continuum and absorption from above. This provides a good starting estimate when measuring all the power spectrum components.
- Lastly we measure all four power spectra $P_{\alpha\alpha}, P_{\beta\beta}, P_{\alpha\beta}, Q_{\alpha\beta}$. This procedure is similar to the one described in [35] but extended to Ly β region.

2.4 Metal contamination at small velocity separations

In [28], it was found that absorption by SiIII contaminates the flux power spectrum measurement. SiIII absorbs at a wavelength 1206.50Å, which is close to the Ly α absorption wavelength, therefore SiIII “shadows” the Ly α correlations in the forest. In principle, one could treat the SiIII absorptions in exactly the same manner as the Ly β absorptions - by writing a full model for this contamination.

While this is possible, it is certainly not easy, because any estimator will have a difficult time distinguishing between the two absorptions. The most likely result would be heavily correlated measurements between SiIII and Ly α power. Therefore, it is easier to treat the SiIII absorption as a small correction to the Ly α absorption.

We will later find a similar contamination issue in the Ly β forest. Both contaminations leak power into $P_{\alpha\beta}$ and $Q_{\alpha\beta}$. Fortunately, the cross-correlations are able to distinguish between the relative signs of these absorptions.

We therefore develop a simple model with one contaminant in the Ly α forest and one dominant in the Ly β forest.

The basic assumption of this model is that the fluctuations of the metal contaminant can be modeled as a scaled and shifted flux fluctuation field of the Ly α (or Ly β) field [28]

$$\delta'_\alpha(x) = \delta_\alpha(x) + \delta_M(x) = \delta_\alpha(x) + a\delta_\alpha(x + v_\alpha). \quad (2.26)$$

As discussed in the Section 2.2, this approximation does eventually break down at some level of precision, but it does provide a good fit to the data. For a more detailed analysis of metal contaminations see [15].

This model of flux fluctuations yields the following power spectrum

$$P'_{\alpha\alpha}(k) = P_{\alpha\alpha}(k) [1 + a^2 + 2a \cos(kv_\alpha)] . \quad (2.27)$$

and ditto for the Ly β power spectrum contaminated with a metal of strength b and frequency v_β .

In the cross-power spectrum, this model affects both the real and imaginary components of the cross power spectrum

$$P'_{\alpha\beta}(k) = n(k)P_{\alpha\beta}(k) + m(k)Q_{\alpha\beta}(k), \quad (2.28)$$

$$Q'_{\alpha\beta}(k) = n(k)Q_{\alpha\beta}(k) - m(k)P_{\alpha\beta}(k), \quad (2.29)$$

where the functions $n(k)$ and $m(k)$ are given by

$$n(k) = 1 + a \cos(kv_\alpha) + b \cos(kv_\beta) + ab \cos[k(v_\beta - v_\alpha)], \quad (2.30)$$

$$m(k) = a \sin(kv_\alpha) - b \sin(kv_\beta) - ab \sin[k(v_\beta - v_\alpha)]. \quad (2.31)$$

The metal contaminant mixes the intrinsic real and imaginary part of the cross power. This means that even if there would have been no intrinsic imaginary power one would still measure non-zero contribution of the imaginary cross power spectrum. This conclusion makes sense intuitively. $Q_{\alpha\beta} = 0$ requires the distribution of Ly α and Ly β absorptions to be symmetrical with respect to the inversion of the radial axis; a metal absorption at a small separation with a fixed sign will naturally break this symmetry.

Finally, we note that *for this particular model* of metal contamination, the contamination cancels perfectly for the cross-correlation coefficient defined as in Equation 2.15.

3 Data & Synthetic data

In this work we use BOSS quasars from the Data Release 9 (DR9; [1]) sample. The quasar target selection for the DR9 sample of BOSS observations is described in detail in [33] and we refer reader to that publication for the details.

We model continuum over the rest frame wavelength range of 978Å to 1600Å. This region is the same as in Ly α analysis of the paper Slosar et al. ([35]) but is extended to lower rest frame wavelengths to enclose the Ly β forest. For the purpose of our analysis we define the Ly α forest to be 1041 – 1185Å, which is similar to the range used by McDonald et al. ([27]) and more conservative than the range in [35]. The upper limit for the Ly α forest

is thus roughly in the regime where proximity effects and Ly α emission line profile can be assumed to be small. For similar reasons, the lower limit is also kept a safe distance away from the Ly β emission peak.

In similar spirit we define the Ly β forest region as rest frame 978 – 1014Å. This range is a bit more conservative than the Ly α range, since the Lyman emission peaks become narrower as one moves long the series (i.e. Ly β emission peak is narrower than Ly α emission peak). The Ly β forest range covers a much shorter path length than the Ly α region, which means inherently less signal. Also, we reiterate that while there is only Ly α absorption in the Ly α forest region defined in this paper, there are both Ly α and Ly β absorptions in the Ly β forest region. Of course, there is metal contamination throughout both forests.

3.1 Mock data

We tested our technique on the same mock data as used in [14, 35]. It is important to stress this mock data-set is not optimal for testing this analysis, since it is focused on the three-dimensional correlations. The small scale power is roughly correct, but only at an order-of-magnitude level. Since we are not aiming at precision cosmology, this should not be a major handicap for our study. If one demonstrates that we can measure the power spectrum without a major bias in these mock data-sets, we are also likely to be making reliable measurements in the true data.

To extend the mock data used in [35] to the Ly β forest, we scaled the optical depth in the τ_α field by $r_{\beta\alpha}$ (see Equation (1.2)) and translated it to an appropriate redshift. The Principal Component Analysis (PCA) continua do not extend to these low redshifts and so we artificially extend them with a constant value.

4 Application to mock data

We tested our analysis on the mock data as follows. First, we demonstrated that our quadratic estimator yields an unbiased result for a white noise input signal which perfectly cross-correlates α and β fields. Next we applied our estimator to the mock data-set, assuming perfect knowledge of the continuum and mean absorption. These results were compared with the full analysis, in which we infer all the quantities from the data, as we must do with the real data. We present these results in Figures 2 and 3.

Figure 2 shows the inferred mean absorption from the mock data-set for both Ly α and Ly β , together with real measurements discussed in the next section. For this section, the relevant plot is Figure 3, which shows how fitting for the continuum fluctuations affects the measured power spectra. Small disagreements are consistent with the fact that the mock data-set misreports the noise-levels to mimic our real misunderstanding of the noise properties of spectrograph (see section 2.2 of [35]). We have also performed simpler tests for which we assumed the Ly α forest field to be perfectly white, fit the data with a single power spectrum bin and compared this with direct estimates using variances - this test convinced us that we do not have missing pre-factors in our estimator. However, we have not carefully tested redshift-interpolation and other more subtle aspects of the estimator.

These tests lead us to conclude that our data analysis will be able to reconstruct the measured power spectrum at the level of precision relevant for this exploratory work when applied to the real data.

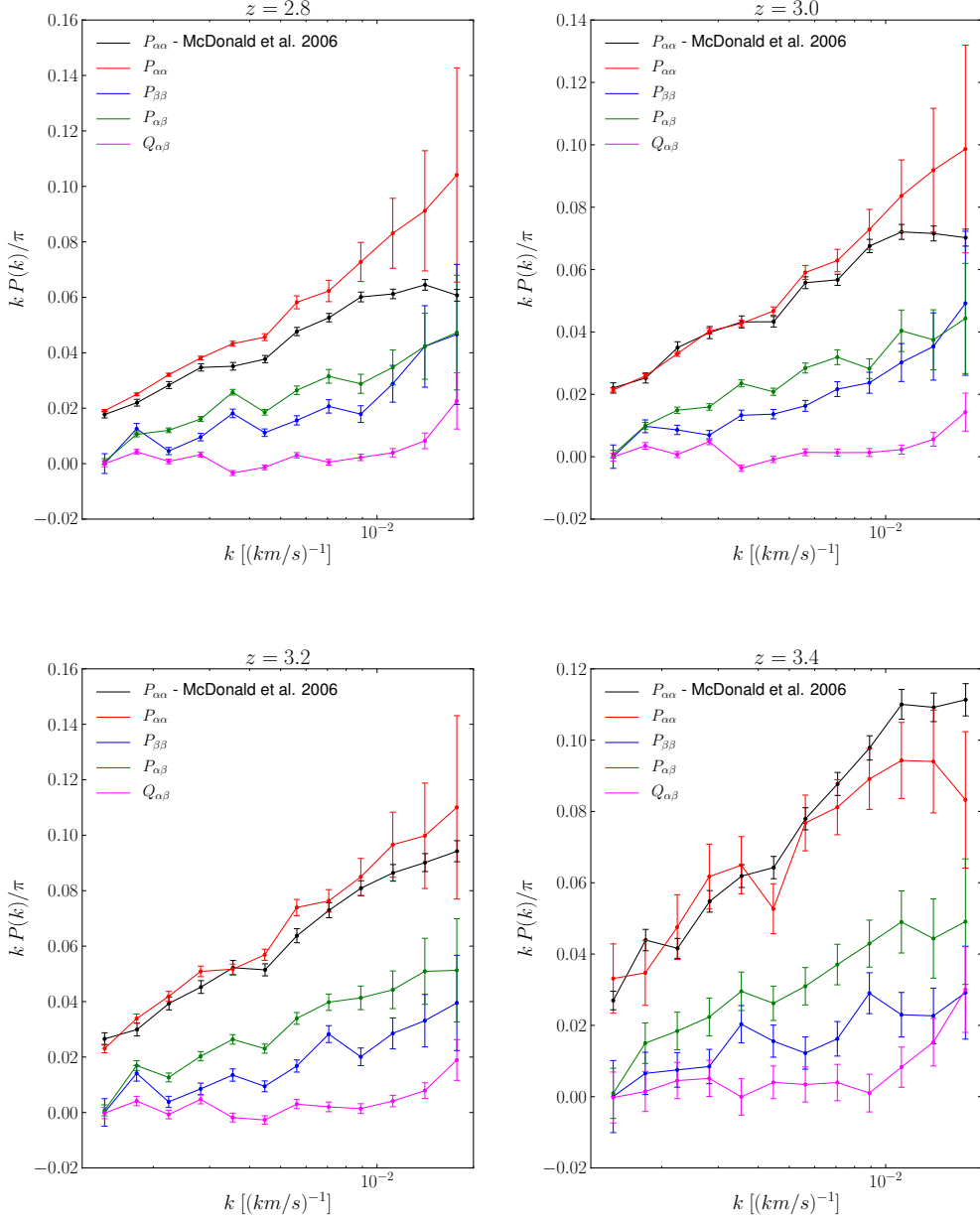


Figure 5. Measured power spectrum components: Ly α power spectrum (red), Ly β power spectrum (blue), real (green) and imaginary (magenta) part of the cross power spectrum. It can be clearly seen that both Ly α and real part of the cross power spectrum are detected with high significance while the imaginary part has lowest detection significance. Also apparent are oscillations in all four components.

5 Results

We applied our data reduction method to the data. Much of the analysis is common with [35] and we refer the reader to that publication for more details. In Figure 2 we plot \bar{F} for Ly α and Ly β forests in mock data and real data. The absolute normalization of each individual mean absorption is arbitrary (since it is degenerate with the mean continuum shape in the relevant forest regions). The error bars are underestimated, since they do not correctly take into account correlations between pixels. Nevertheless, the visual agreement between the results on the mock data and real data is quite good and, in fact, better than one would naively expect given that the small scale power is not appropriately reproduced in these mock data.

Next we discuss the covariance matrix of our measurements. In the top row of Figure 4 we show the covariance matrices derived from the optimal estimator and the data. The covariance matrix has the expected structure. Measurements of the Ly α power spectrum are effectively uncorrelated, with only weak anti-correlation between adjacent bins. Measurements of the Ly β power spectra are similar, but the anti-correlations between adjacent bins are larger, since the available path length is smaller. Measurement of the cross-power spectra are also only weakly internally correlated, but they show significant correlations with both auto power spectra. The most interesting aspect is the covariance structure of the $Q_{\alpha\beta}$ with $P_{\alpha\beta}$, where bins at the same k are uncorrelated, but are somewhat correlated with adjacent k -bins.

Measurements of the 1D quantities in the data are conveniently bootstrapped by assuming each quasar to be an independent measurement of this quantity (this should be an excellent approximation). We generated 3000 bootstrap samples of our dataset and calculated the corresponding bootstrap covariance matrix. When compared with the bootstrap derived covariance matrix, the estimator under-estimates the diagonal elements of the covariance matrix by approximately 10%. We correct for this error in subsequent use of the matrix by multiplying all element of the covariance matrix by 1.1. The correlation structure for this matrix is displayed in the bottom row of Figure 4. We see that compared to the estimator matrix, the structure is in general similar. One important difference is that the bootstrapping is selecting a constant-like contribution to variance in the auto-correlations. This feature likely arises due to our imperfect fitting of the quasar amplitude for small signal-to-noise quasars that modulates the power spectrum normalization.

So far, for example in mock-testing, we have completely neglected the effect of the finite spectrograph resolution. We proceed to make a rough correction as follows. We estimate our beam correction as a mean over pairs of pixels that contribute in the same (k, z) bin. The errors on the spectrograph resolution are estimated to be of order of 10% ([30]). This results in a substantial increase in the size of the error-bars in our measurements at high k .

In Figure 5 we compare our measurements and the measurements of the Ly α forest alone using 3000 SDSS quasars by [27]. In general, we find good agreement, except at the lowest redshift bin, where we measure excess power when compared to the McDonald et al measurements. The most likely explanation for mismatch is poor noise modeling in our data, since it is known that the pipeline noise is not accurate [35].

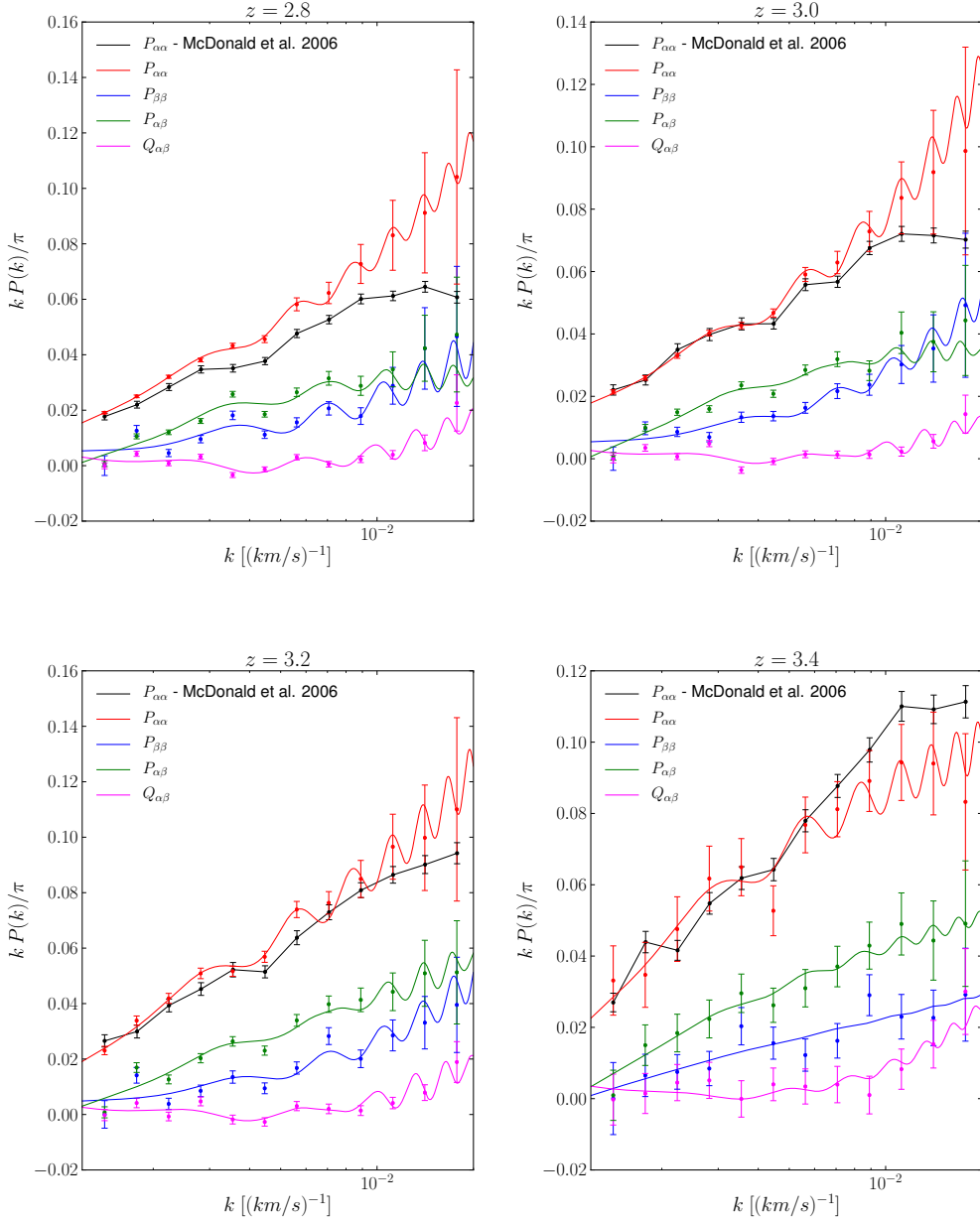


Figure 6. Fits for power spectrum models with metal contaminants in Ly α and Ly β forest. The model does not produce a good fit to the data, but the oscillation frequencies are measured very robustly.

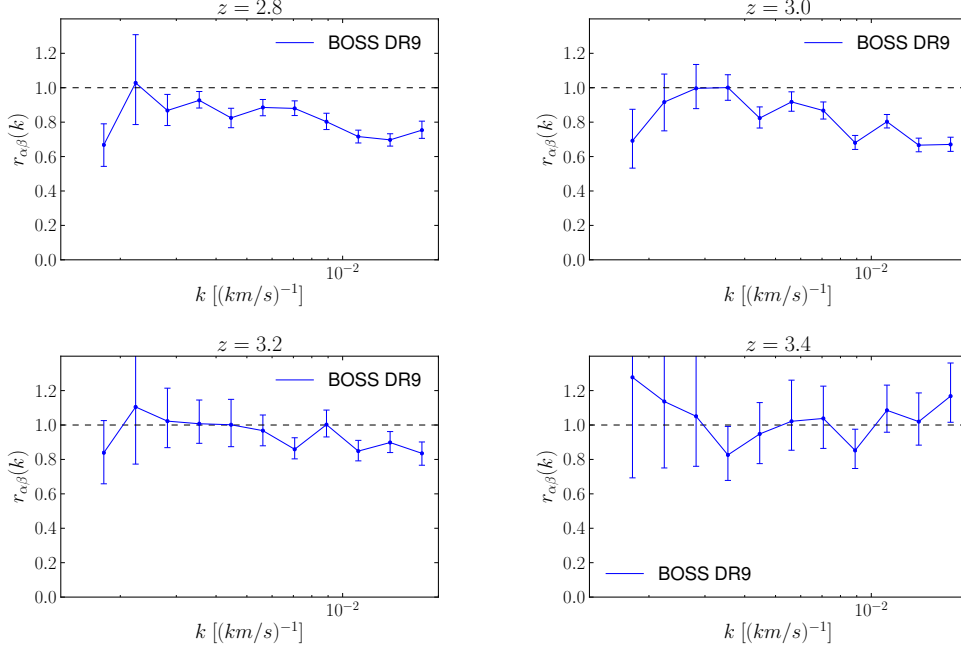


Figure 7. Measured cross correlation coefficient (2.15) from the data. Within the error bars, the coefficient is constant on large scales and is falling off towards smaller scales.

From Fig. 5 it is apparent that oscillations are imprinted on top of a smooth power spectrum. We propose that these oscillations are best described as being due to the presence of contaminating metal at small separation from the main absorption line ([27]).

In order to test this hypothesis, we fit our data as an intrinsically smooth power spectrum described by a 2nd order polynomial fit in $\log(k)$. All four components ($P_{\alpha\alpha}$, $P_{\beta\beta}$, $P_{\alpha\beta}$, $Q_{\alpha\beta}$) were fit with independent smooth component at each redshifts. We convolved this model with a dominant metal contamination at fixed separation as described in the section 2.4. We assumed that contaminating oscillation strength is independent in each redshift bin, but that the oscillation frequencies (v_α and v_β) are fixed.

The best-fit model resulting from this procedure can be found in Figure 6. This model did not produce a good fit to the data - in fact our best fit gives $\chi^2 = 299.92$ with 134 degrees of freedom (even after correcting for the 10% error-covariance underestimate). Not surprisingly, we have found that the two robustly measured quantities are the oscillation frequencies of the contaminating components, which are given by

$$v_\alpha = 2269 \pm 19 \text{ km s}^{-1}, \quad (5.1)$$

$$v_\beta = -1820 \pm 13 \text{ km s}^{-1}. \quad (5.2)$$

Since we do not produce a good fit to the data, the error bars are likely underestimated. Nevertheless, we can identify the contaminants. The metal contaminant in Ly α forest (v_α) is the SiIII line transition, absorbing at 1206.5Å, which is separated from Ly α by $v_\alpha =$

2271 km s^{-1} confirming results by [27]. The contaminant in the $\text{Ly}\beta$ forest is identified with OVI that absorbs at 1031.9\AA , corresponding to $v_\beta = -1801 \text{ km s}^{-1}$.

We proceed by examining the cross-correlation coefficient defined in Equation 2.15. As mentioned in Section 2.4, under the simplified model of metal contamination, its effect cancels exactly in this quantity. Errors due to absolute noise power that affect the auto power spectra but not the cross power spectra will, in general, affect this quantity. The quantity $r_{\alpha\beta}(k)$ is plotted in Figure (7). The statistical error bars on this plot were derived by drawing samples of power spectra consistent with the measured data and the associated covariance matrix and examining the resulting scatter in r . Although the measurements are uncertain and error bars large, the general behavior follows the expectations. On large scale we see nearly unity cross-correlations that tends to decrease towards smaller scales.

6 Conclusion

In this paper we studied the possibility of measuring the $\text{Ly}\beta$ forest in spectra of quasars. The fact that the underlying density field evolves with redshift breaks the symmetry along the line of sight when measuring cross power spectrum which results in a cross-correlation function that is not symmetric with respect to changing the sign of the velocity difference. This yields an intrinsic non-zero imaginary component to the cross power spectrum. When considering the $\text{Ly}\beta$ in addition to $\text{Ly}\alpha$ forest, one therefore measures three new components. Including higher Lyman transitions will add new auto power spectra and in general two new cross-power spectra for any combination of absorbing lines. However, due to decreasing path-length of higher-order forests, it is not clear whether it is useful to venture beyond the $\text{Ly}\beta$ line.

Measurements of the $\text{Ly}\beta$ power spectrum and the $\text{Ly}\alpha$ - $\text{Ly}\beta$ cross power spectra offer an improved way of estimating cosmological parameters over using the $\text{Ly}\alpha$ power spectrum alone, since we expect that many of the astrophysical nuisance parameters that are degenerate with the cosmologically interesting parameters can be measured semi-independently from the new quantities. This stems from the fact that the two transitions map the same intergalactic medium, but are sensitive to different density and temperature ranges. This presents an opportunity to better constrain IGM parameters of the flux-density transformation and thus break the degeneracies between IGM parameters (especially parameters of the equation of state) and cosmology parameters (e.g. scalar spectral index).

Measurements of the cross power spectra $P_{\alpha\beta}$ are independent of the choice of noise model. With future theoretical modeling, we should be able to predict the cross-correlation coefficient accurately and therefore the cross-power spectra will provide a convincing self-consistency check.

We have measured the quantities discussed above in the BOSS DR9 data. Our work is clearly not accurate at the level required for precision cosmology fits. In particular, effects of noise, spectrograph resolution and metal contamination (both in-forest like OVI, but also lower redshift metals that are uncorrelated with the signal of interest). Along with a better data analysis, the theory also needs to be further investigated using numerical simulations of the $\text{Ly}\beta$ forest. These are trivial to generate from the $\text{Ly}\alpha$ simulations by appropriate rescaling of the optical depth.

Nevertheless, we have measured power in all quantities discussed above with high significance. Our measurements confirm the standard picture describing the $\text{Ly}\alpha$ forest. The cross-correlation coefficient is close to unity on large scales as expected from qualitative ar-

guments. We found oscillations in all the power spectra measured. Our fits indicate that these features are best explained by a combination of the SiIII contamination of the Ly α forest (known previously) and OVI contamination in the Ly β forest (new to this work).

Acknowledgments

Funding for SDSS-III has been provided by the Alfred P. Sloan Foundation, the Participating Institutions, the National Science Foundation, and the U.S. Department of Energy Office of Science. The SDSS-III web site is <http://www.sdss3.org/>.

SDSS-III is managed by the Astrophysical Research Consortium for the Participating Institutions of the SDSS-III Collaboration including the University of Arizona, the Brazilian Participation Group, Brookhaven National Laboratory, University of Cambridge, Carnegie Mellon University, University of Florida, the French Participation Group, the German Participation Group, Harvard University, the Instituto de Astrofísica de Canarias, the Michigan State/Notre Dame/JINA Participation Group, Johns Hopkins University, Lawrence Berkeley National Laboratory, Max Planck Institute for Astrophysics, Max Planck Institute for Extraterrestrial Physics, New Mexico State University, New York University, Ohio State University, Pennsylvania State University, University of Portsmouth, Princeton University, the Spanish Participation Group, University of Tokyo, University of Utah, Vanderbilt University, University of Virginia, University of Washington, and Yale University.

References

- [1] C. P. Ahn, R. Alexandroff, C. Allende Prieto, S. F. Anderson, T. Anderton, B. H. Andrews, É. Aubourg, S. Bailey, E. Balbinot, R. Barnes, and et al. The Ninth Data Release of the Sloan Digital Sky Survey: First Spectroscopic Data from the SDSS-III Baryon Oscillation Spectroscopic Survey. *ApJS*, 203:21, December 2012.
- [2] L. Anderson, E. Aubourg, S. Bailey, F. Beutler, A. S. Bolton, J. Brinkmann, J. R. Brownstein, C.-H. Chuang, A. J. Cuesta, K. S. Dawson, D. J. Eisenstein, K. Honscheid, E. A. Kazin, D. Kirkby, M. Manera, C. K. McBride, O. Mena, R. C. Nichol, M. D. Olmstead, N. Padmanabhan, N. Palanque-Delabrouille, W. J. Percival, F. Prada, A. J. Ross, N. P. Ross, A. G. Sanchez, L. Samushia, D. J. Schlegel, D. P. Schneider, H.-J. Seo, M. A. Strauss, D. Thomas, J. L. Tinker, R. Tojeiro, L. Verde, D. H. Weinberg, X. Xu, and C. Yèche. The clustering of galaxies in the SDSS-III Baryon Oscillation Spectroscopic Survey: Measuring D_A and H at $z=0.57$ from the Baryon Acoustic Peak in the Data Release 9 Spectroscopic Galaxy Sample. *ArXiv e-prints*, March 2013.
- [3] J. Bechtold, A. P. S. Crotts, R. C. Duncan, and Y. Fang. Spectroscopy of the double quasars Q1343+266A, B: A new determination of the size of Lyman-alpha forest absorbers. *ApJL*, 437:L83–L86, December 1994.
- [4] A. S. Bolton, D. J. Schlegel, É. Aubourg, S. Bailey, V. Bhardwaj, J. R. Brownstein, S. Burles, Y.-M. Chen, K. Dawson, D. J. Eisenstein, J. E. Gunn, G. R. Knapp, C. P. Loomis, R. H. Lupton, C. Maraston, D. Muna, A. D. Myers, M. D. Olmstead, N. Padmanabhan, I. Pâris, W. J. Percival, P. Petitjean, C. M. Rockosi, N. P. Ross, D. P. Schneider, Y. Shu, M. A. Strauss, D. Thomas, C. A. Tremonti, D. A. Wake, B. A. Weaver, and W. M. Wood-Vasey. Spectral Classification and Redshift Measurement for the SDSS-III Baryon Oscillation Spectroscopic Survey. *AJ*, 144:144, November 2012.
- [5] J. Bovy, J. F. Hennawi, D. W. Hogg, A. D. Myers, J. A. Kirkpatrick, D. J. Schlegel, N. P. Ross, E. S. Sheldon, I. D. McGreer, D. P. Schneider, and B. A. Weaver. Think Outside the

Color Box: Probabilistic Target Selection and the SDSS-XDQSO Quasar Targeting Catalog. *ApJ*, 729:141, March 2011.

- [6] N. G. Busca, T. Delubac, J. Rich, S. Bailey, A. Font-Ribera, D. Kirkby, J.-M. Le Goff, M. M. Pieri, A. Slosar, É. Aubourg, J. E. Bautista, D. Bizyaev, M. Blomqvist, A. S. Bolton, J. Bovy, H. Brewington, A. Borde, J. Brinkmann, B. Carithers, R. A. C. Croft, K. S. Dawson, G. Ebelke, D. J. Eisenstein, J.-C. Hamilton, S. Ho, D. W. Hogg, K. Honscheid, K.-G. Lee, B. Lundgren, E. Malanushenko, V. Malanushenko, D. Margala, C. Maraston, K. Mehta, J. Miralda-Escudé, A. D. Myers, R. C. Nichol, P. Noterdaeme, M. D. Olmstead, D. Oravetz, N. Palanque-Delabrouille, K. Pan, I. Pâris, W. J. Percival, P. Petitjean, N. A. Roe, E. Rollinde, N. P. Ross, G. Rossi, D. J. Schlegel, D. P. Schneider, A. Shelden, E. S. Sheldon, A. Simmons, S. Snedden, J. L. Tinker, M. Viel, B. A. Weaver, D. H. Weinberg, M. White, C. Yèche, and D. G. York. Baryon acoustic oscillations in the Ly α forest of BOSS quasars. *A&A*, 552:A96, April 2013.
- [7] R. Cen, J. Miralda-Escudé, J. P. Ostriker, and M. Rauch. Gravitational collapse of small-scale structure as the origin of the Lyman-alpha forest. *ApJL*, 437:L9–L12, December 1994.
- [8] R. A. C. Croft, D. H. Weinberg, M. Bolte, S. Burles, L. Hernquist, N. Katz, D. Kirkman, and D. Tytler. Toward a Precise Measurement of Matter Clustering: Ly α Forest Data at Redshifts 2-4. *ApJ*, 581:20–52, December 2002.
- [9] R. A. C. Croft, D. H. Weinberg, N. Katz, and L. Hernquist. Recovery of the Power Spectrum of Mass Fluctuations from Observations of the Ly alpha Forest. *ApJ*, 495:44, March 1998.
- [10] K. S. Dawson, D. J. Schlegel, C. P. Ahn, S. F. Anderson, É. Aubourg, S. Bailey, R. H. Barkhouser, J. E. Bautista, A. Beifiori, A. A. Berlind, V. Bhardwaj, D. Bizyaev, C. H. Blake, M. R. Blanton, M. Blomqvist, A. S. Bolton, A. Borde, J. Bovy, W. N. Brandt, H. Brewington, J. Brinkmann, P. J. Brown, J. R. Brownstein, K. Bundy, N. G. Busca, W. Carithers, A. R. Carnero, M. A. Carr, Y. Chen, J. Comparat, N. Connolly, F. Cope, R. A. C. Croft, A. J. Cuesta, L. N. da Costa, J. R. A. Davenport, T. Delubac, R. de Putter, S. Dhital, A. Ealet, G. L. Ebelke, D. J. Eisenstein, S. Escoffier, X. Fan, N. Filiz Ak, H. Finley, A. Font-Ribera, R. Génova-Santos, J. E. Gunn, H. Guo, D. Haggard, P. B. Hall, J.-C. Hamilton, B. Harris, D. W. Harris, S. Ho, D. W. Hogg, D. Holder, K. Honscheid, J. Huehnerhoff, B. Jordan, W. P. Jordan, G. Kauffmann, E. A. Kazin, D. Kirkby, M. A. Klaene, J.-P. Kneib, J.-M. Le Goff, K.-G. Lee, D. C. Long, C. P. Loomis, B. Lundgren, R. H. Lupton, M. A. G. Maia, M. Makler, E. Malanushenko, V. Malanushenko, R. Mandelbaum, M. Manera, C. Maraston, D. Margala, K. L. Masters, C. K. McBride, P. McDonald, I. D. McGreer, R. G. McMahon, O. Mena, J. Miralda-Escudé, A. D. Montero-Dorta, F. Montesano, D. Muna, A. D. Myers, T. Naugle, R. C. Nichol, P. Noterdaeme, S. E. Nuza, M. D. Olmstead, A. Oravetz, D. J. Oravetz, R. Owen, N. Padmanabhan, N. Palanque-Delabrouille, K. Pan, J. K. Parejko, I. Pâris, W. J. Percival, I. Pérez-Fournon, I. Pérez-Ràfols, P. Petitjean, R. Pfaffenberger, J. Pforr, M. M. Pieri, F. Prada, A. M. Price-Whelan, M. J. Raddick, R. Rebolo, J. Rich, G. T. Richards, C. M. Rockosi, N. A. Roe, A. J. Ross, N. P. Ross, G. Rossi, J. A. Rubiño-Martin, L. Samushia, A. G. Sánchez, C. Sayres, S. J. Schmidt, D. P. Schneider, C. G. Scóccola, H.-J. Seo, A. Shelden, E. Sheldon, Y. Shen, Y. Shu, A. Slosar, S. A. Smee, S. A. Snedden, F. Stauffer, O. Steele, M. A. Strauss, A. Streblyanska, N. Suzuki, M. E. C. Swanson, T. Tal, M. Tanaka, D. Thomas, J. L. Tinker, R. Tojeiro, C. A. Tremonti, M. Vargas Magaña, L. Verde, M. Viel, D. A. Wake, M. Watson, B. A. Weaver, D. H. Weinberg, B. J. Weiner, A. A. West, M. White, W. M. Wood-Vasey, C. Yèche, I. Zehavi, G.-B. Zhao, and Z. Zheng. The Baryon Oscillation Spectroscopic Survey of SDSS-III. *AJ*, 145:10, January 2013.
- [11] M. Dijkstra, A. Lidz, and L. Hui. Beyond Ly α : Constraints and Consistency Tests from the Ly β Forest. *ApJ*, 605:7–13, April 2004.
- [12] D. J. Eisenstein, D. H. Weinberg, E. Agol, H. Aihara, C. Allende Prieto, S. F. Anderson, J. A. Arns, É. Aubourg, S. Bailey, E. Balbinot, and et al. SDSS-III: Massive Spectroscopic Surveys

of the Distant Universe, the Milky Way, and Extra-Solar Planetary Systems. *AJ*, 142:72, September 2011.

- [13] D. J. Eisenstein, I. Zehavi, D. W. Hogg, R. Scoccimarro, M. R. Blanton, R. C. Nichol, R. Scranton, H.-J. Seo, M. Tegmark, Z. Zheng, S. F. Anderson, J. Annis, N. Bahcall, J. Brinkmann, S. Burles, F. J. Castander, A. Connolly, I. Csabai, M. Doi, M. Fukugita, J. A. Frieman, K. Glazebrook, J. E. Gunn, J. S. Hendry, G. Hennessy, Z. Ivezić, S. Kent, G. R. Knapp, H. Lin, Y.-S. Loh, R. H. Lupton, B. Margon, T. A. McKay, A. Meiksin, J. A. Munn, A. Pope, M. W. Richmond, D. Schlegel, D. P. Schneider, K. Shimasaku, C. Stoughton, M. A. Strauss, M. SubbaRao, A. S. Szalay, I. Szapudi, D. L. Tucker, B. Yanny, and D. G. York. Detection of the Baryon Acoustic Peak in the Large-Scale Correlation Function of SDSS Luminous Red Galaxies. *ApJ*, 633:560–574, November 2005.
- [14] A. Font-Ribera, P. McDonald, and J. Miralda-Escudé. Generating mock data sets for large-scale Lyman- α forest correlation measurements. *JCAP*, 1:1, January 2012.
- [15] A. Font-Ribera and J. Miralda-Escudé. The effect of high column density systems on the measurement of the Lyman- α forest correlation function. *JCAP*, 7:28, July 2012.
- [16] M. Fukugita, T. Ichikawa, J. E. Gunn, M. Doi, K. Shimasaku, and D. P. Schneider. The Sloan Digital Sky Survey Photometric System. *AJ*, 111:1748, April 1996.
- [17] A. Garzilli, J. S. Bolton, T.-S. Kim, S. Leach, and M. Viel. The intergalactic medium thermal history at redshift $z=1.7$ – 3.2 from the Lyman alpha forest: a comparison of measurements using wavelets and the flux distribution. *ArXiv e-prints*, February 2012.
- [18] J. E. Gunn, M. Carr, C. Rockosi, M. Sekiguchi, K. Berry, B. Elms, E. de Haas, Ž. Ivezić, G. Knapp, R. Lupton, G. Pauls, R. Simcoe, R. Hirsch, D. Sanford, S. Wang, D. York, F. Harris, J. Annis, L. Bartozek, W. Boroski, J. Bakken, M. Haldeman, S. Kent, S. Holm, D. Holmgren, D. Petravick, A. Prosapio, R. Rechenmacher, M. Doi, M. Fukugita, K. Shimasaku, N. Okada, C. Hull, W. Siegmund, E. Mannery, M. Blouke, D. Heidtman, D. Schneider, R. Lucinio, and J. Brinkman. The Sloan Digital Sky Survey Photometric Camera. *AJ*, 116:3040–3081, December 1998.
- [19] J. E. Gunn and B. A. Peterson. On the Density of Neutral Hydrogen in Intergalactic Space. *ApJ*, 142:1633–1641, November 1965.
- [20] J. E. Gunn, W. A. Siegmund, E. J. Mannery, R. E. Owen, C. L. Hull, R. F. Leger, L. N. Carey, G. R. Knapp, D. G. York, W. N. Boroski, S. M. Kent, R. H. Lupton, C. M. Rockosi, M. L. Evans, P. Waddell, J. E. Anderson, J. Annis, J. C. Barentine, L. M. Bartoszek, S. Bastian, S. B. Bracker, H. J. Brewington, C. I. Briegel, J. Brinkmann, Y. J. Brown, M. A. Carr, P. C. Czarapata, C. C. Drennan, T. Dombeck, G. R. Federwitz, B. A. Gillespie, C. Gonzales, S. U. Hansen, M. Harvanek, J. Hayes, W. Jordan, E. Kinney, M. Klaene, S. J. Kleinman, R. G. Kron, J. Kresinski, G. Lee, S. Limmongkol, C. W. Lindenmeyer, D. C. Long, C. L. Loomis, P. M. McGehee, P. M. Mantsch, E. H. Neilsen, Jr., R. M. Neswold, P. R. Newman, A. Nitta, J. Peoples, Jr., J. R. Pier, P. S. Prieto, A. Prosapio, C. Rivetta, D. P. Schneider, S. Snedden, and S.-i. Wang. The 2.5 m Telescope of the Sloan Digital Sky Survey. *AJ*, 131:2332–2359, April 2006.
- [21] D. Kirkby, D. Margala, A. Slosar, S. Bailey, N. G. Busca, T. Delubac, J. Rich, J. E. Bautista, M. Blomqvist, J. R. Brownstein, B. Carithers, R. A. C. Croft, K. S. Dawson, A. Font-Ribera, J. Miralda-Escudé, A. D. Myers, R. C. Nichol, N. Palanque-Delabrouille, I. Pâris, P. Petitjean, G. Rossi, D. J. Schlegel, D. P. Schneider, M. Viel, D. H. Weinberg, and C. Yèche. Fitting methods for baryon acoustic oscillations in the Lyman- α forest fluctuations in BOSS data release 9. *JCAP*, 3:24, March 2013.
- [22] K.-G. Lee, S. Bailey, L. E. Bartsch, W. Carithers, K. S. Dawson, D. Kirkby, B. Lundgren, D. Margala, N. Palanque-Delabrouille, M. M. Pieri, D. J. Schlegel, D. H. Weinberg, C. Yèche, É. Aubourg, J. Bautista, D. Bizyaev, M. Blomqvist, A. S. Bolton, A. Borde, H. Brewington,

- N. G. Busca, R. A. C. Croft, T. Delubac, G. Ebelke, D. J. Eisenstein, A. Font-Ribera, J. Ge, J.-C. Hamilton, J. F. Hennawi, S. Ho, K. Honscheid, J.-M. Le Goff, E. Malanushenko, V. Malanushenko, J. Miralda-Escudé, A. D. Myers, P. Noterdaeme, D. Oravetz, K. Pan, I. Pâris, P. Petitjean, J. Rich, E. Rollinde, N. P. Ross, G. Rossi, D. P. Schneider, A. Simmons, S. Snedden, A. Slosar, D. N. Spergel, N. Suzuki, M. Viel, and B. A. Weaver. The BOSS Ly α Forest Sample from SDSS Data Release 9. *AJ*, 145:69, March 2013.
- [23] R. Lynds. The Absorption-Line Spectrum of 4c 05.34. *ApJL*, 164:L73, March 1971.
- [24] R. Mandelbaum, P. McDonald, U. Seljak, and R. Cen. Precision cosmology from the Lyman α forest: power spectrum and bispectrum. *MNRAS*, 344:776–788, September 2003.
- [25] P. McDonald. Toward a Measurement of the Cosmological Geometry at $z \sim 2$: Predicting Ly α Forest Correlation in Three Dimensions and the Potential of Future Data Sets. *ApJ*, 585:34–51, March 2003.
- [26] P. McDonald, J. Miralda-Escudé, M. Rauch, W. L. W. Sargent, T. A. Barlow, R. Cen, and J. P. Ostriker. The Observed Probability Distribution Function, Power Spectrum, and Correlation Function of the Transmitted Flux in the Ly α Forest. *ApJ*, 543:1–23, November 2000.
- [27] P. McDonald, U. Seljak, S. Burles, D. J. Schlegel, D. H. Weinberg, R. Cen, D. Shih, J. Schaye, D. P. Schneider, N. A. Bahcall, J. W. Briggs, J. Brinkmann, R. J. Brunner, M. Fukugita, J. E. Gunn, Ž. Ivezić, S. Kent, R. H. Lupton, and D. E. Vanden Berk. The Ly α Forest Power Spectrum from the Sloan Digital Sky Survey. *ApJS*, 163:80–109, March 2006.
- [28] P. McDonald, U. Seljak, R. Cen, D. Shih, D. H. Weinberg, S. Burles, D. P. Schneider, D. J. Schlegel, N. A. Bahcall, J. W. Briggs, J. Brinkmann, M. Fukugita, Ž. Ivezić, S. Kent, and D. E. Vanden Berk. The Linear Theory Power Spectrum from the Ly α Forest in the Sloan Digital Sky Survey. *ApJ*, 635:761–783, December 2005.
- [29] P. Noterdaeme, P. Petitjean, W. C. Carithers, I. Pâris, A. Font-Ribera, S. Bailey, E. Aubourg, D. Bizyaev, G. Ebelke, H. Finley, J. Ge, E. Malanushenko, V. Malanushenko, J. Miralda-Escudé, A. D. Myers, D. Oravetz, K. Pan, M. M. Pieri, N. P. Ross, D. P. Schneider, A. Simmons, and D. G. York. Column density distribution and cosmological mass density of neutral gas: Sloan Digital Sky Survey-III Data Release 9. *A&A*, 547:L1, November 2012.
- [30] N. Palanque-Delabrouille, C. Yèche, A. Borde, J.-M. Le Goff, G. Rossi, M. Viel, É. Aubourg, S. Bailey, J. Bautista, M. Blomqvist, A. Bolton, J. S. Bolton, N. G. Busca, B. Carithers, R. A. C. Croft, K. S. Dawson, T. Delubac, A. Font-Ribera, S. Ho, D. Kirkby, K.-G. Lee, D. Margala, J. Miralda-Escudé, D. Muna, A. D. Myers, P. Noterdaeme, I. Pâris, P. Petitjean, M. M. Pieri, J. Rich, E. Rollinde, N. P. Ross, D. J. Schlegel, D. P. Schneider, A. Slosar, and D. H. Weinberg. The one-dimensional Ly-alpha forest power spectrum from BOSS. *ArXiv e-prints*, June 2013.
- [31] I. Pâris, P. Petitjean, É. Aubourg, S. Bailey, N. P. Ross, A. D. Myers, M. A. Strauss, S. F. Anderson, E. Arnau, J. Bautista, D. Bizyaev, A. S. Bolton, J. Bovy, W. N. Brandt, H. Brewington, J. R. Browstein, N. Busca, D. Capellupo, W. Carithers, R. A. C. Croft, K. Dawson, T. Delubac, G. Ebelke, D. J. Eisenstein, P. Engelke, X. Fan, N. Filiz Ak, H. Finley, A. Font-Ribera, J. Ge, R. R. Gibson, P. B. Hall, F. Hamann, J. F. Hennawi, S. Ho, D. W. Hogg, Ž. Ivezić, L. Jiang, A. E. Kimball, D. Kirkby, J. A. Kirkpatrick, K.-G. Lee, J.-M. Le Goff, B. Lundgren, C. L. MacLeod, E. Malanushenko, V. Malanushenko, C. Maraston, I. D. McGreer, R. G. McMahon, J. Miralda-Escudé, D. Muna, P. Noterdaeme, D. Oravetz, N. Palanque-Delabrouille, K. Pan, I. Perez-Fournon, M. M. Pieri, G. T. Richards, E. Rollinde, E. S. Sheldon, D. J. Schlegel, D. P. Schneider, A. Slosar, A. Shelden, Y. Shen, A. Simmons, S. Snedden, N. Suzuki, J. Tinker, M. Viel, B. A. Weaver, D. H. Weinberg, M. White, W. M. Wood-Vasey, and C. Yèche. The Sloan Digital Sky Survey quasar catalog: ninth data release. *A&A*, 548:A66, December 2012.
- [32] A. K. Pradhan and S. N. Nahar. *Atomic Astrophysics and Spectroscopy*. Cambridge University

Press, January 2011.

- [33] N. P. Ross, A. D. Myers, E. S. Sheldon, C. Yèche, M. A. Strauss, J. Bovy, J. A. Kirkpatrick, G. T. Richards, É. Aubourg, M. R. Blanton, W. N. Brandt, W. C. Carithers, R. A. C. Croft, R. da Silva, K. Dawson, D. J. Eisenstein, J. F. Hennawi, S. Ho, D. W. Hogg, K.-G. Lee, B. Lundgren, R. G. McMahon, J. Miralda-Escudé, N. Palanque-Delabrouille, I. Pâris, P. Petitjean, M. M. Pieri, J. Rich, N. A. Roe, D. Schiminovich, D. J. Schlegel, D. P. Schneider, A. Slosar, N. Suzuki, J. L. Tinker, D. H. Weinberg, A. Weyant, M. White, and W. M. Wood-Vasey. The SDSS-III Baryon Oscillation Spectroscopic Survey: Quasar Target Selection for Data Release Nine. *ApJS*, 199:3, March 2012.
- [34] A. Slosar, A. Font-Ribera, M. M. Pieri, J. Rich, J.-M. Le Goff, É. Aubourg, J. Brinkmann, N. Busca, B. Carithers, R. Charlassier, M. Cortès, R. Croft, K. S. Dawson, D. Eisenstein, J.-C. Hamilton, S. Ho, K.-G. Lee, R. Lupton, P. McDonald, B. Medolin, D. Muna, J. Miralda-Escudé, A. D. Myers, R. C. Nichol, N. Palanque-Delabrouille, I. Pâris, P. Petitjean, Y. Piškur, E. Rollinde, N. P. Ross, D. J. Schlegel, D. P. Schneider, E. Sheldon, B. A. Weaver, D. H. Weinberg, C. Yèche, and D. G. York. The Lyman- α forest in three dimensions: measurements of large scale flux correlations from BOSS 1st-year data. *JCAP*, 9:1, September 2011.
- [35] A. Slosar, V. Iršič, D. Kirkby, S. Bailey, N. G. Busca, T. Delubac, J. Rich, É. Aubourg, J. E. Bautista, V. Bhardwaj, M. Blomqvist, A. S. Bolton, J. Bovy, J. Brownstein, B. Carithers, R. A. C. Croft, K. S. Dawson, A. Font-Ribera, J.-M. Le Goff, S. Ho, K. Honscheid, K.-G. Lee, D. Margala, P. McDonald, B. Medolin, J. Miralda-Escudé, A. D. Myers, R. C. Nichol, P. Noterdaeme, N. Palanque-Delabrouille, I. Pâris, P. Petitjean, M. M. Pieri, Y. Piškur, N. A. Roe, N. P. Ross, G. Rossi, D. J. Schlegel, D. P. Schneider, N. Suzuki, E. S. Sheldon, U. Seljak, M. Viel, D. H. Weinberg, and C. Yèche. Measurement of baryon acoustic oscillations in the Lyman- α forest fluctuations in BOSS data release 9. *JCAP*, 4:26, April 2013.
- [36] S. Smee, J. E. Gunn, A. Uomoto, N. Roe, D. Schlegel, C. M. Rockosi, M. A. Carr, F. Leger, K. S. Dawson, M. D. Olmstead, J. Brinkmann, R. Owen, R. H. Barkhouser, K. Honscheid, P. Harding, D. Long, R. H. Lupton, C. Loomis, L. Anderson, J. Annis, M. Bernardi, V. Bhardwaj, D. Bizyaev, A. S. Bolton, H. Brewington, J. W. Briggs, S. Burles, J. G. Burns, F. Castander, A. Connolly, J. R. Davenport, G. Ebelke, H. Epps, P. D. Feldman, S. Friedman, J. Frieman, T. Heckman, C. L. Hull, G. R. Knapp, D. M. Lawrence, J. Loveday, E. J. Mannery, E. Malanushenko, V. Malanushenko, A. Merrelli, D. Muna, P. Newman, R. C. Nichol, D. Oravetz, K. Pan, A. C. Pope, P. G. Ricketts, A. Shelden, D. Sandford, W. Siegmund, A. Simmons, D. Smith, S. Snedden, D. P. Schneider, M. Strauss, M. SubbaRao, C. Tremonti, P. Waddell, and D. G. York. The Multi-Object, Fiber-Fed Spectrographs for SDSS and the Baryon Oscillation Spectroscopic Survey. *ArXiv e-prints*, August 2012.
- [37] M. Viel, J. Weller, and M. G. Haehnelt. Constraints on the primordial power spectrum from high-resolution Lyman α forest spectra and WMAP. *MNRAS*, 355:L23–L28, December 2004.
- [38] S. S. Vogt, S. L. Allen, B. C. Bigelow, L. Bresee, B. Brown, T. Cantrall, A. Conrad, M. Couture, C. Delaney, H. W. Epps, D. Hilyard, D. F. Hilyard, E. Horn, N. Jern, D. Kanto, M. J. Keane, R. I. Kibrick, J. W. Lewis, J. Osborne, G. H. Pardeilhan, T. Pfister, T. Ricketts, L. B. Robinson, R. J. Stover, D. Tucker, J. Ward, and M. Z. Wei. HIRES: the high-resolution echelle spectrometer on the Keck 10-m Telescope. In D. L. Crawford & E. R. Craine, editor, *Society of Photo-Optical Instrumentation Engineers (SPIE) Conference Series*, volume 2198 of *Society of Photo-Optical Instrumentation Engineers (SPIE) Conference Series*, page 362, June 1994.
- [39] D. H. Weinberg, R. Davé, N. Katz, and J. A. Kollmeier. The Lyman- α Forest as a Cosmological Tool. In S. H. Holt & C. S. Reynolds, editor, *The Emergence of Cosmic Structure*, volume 666 of *American Institute of Physics Conference Series*, pages 157–169, May 2003.
- [40] M. White. The Ly-a forest. In *The Davis Meeting On Cosmic Inflation*, March 2003.

- [41] D. G. York, J. Adelman, J. E. Anderson, Jr., S. F. Anderson, J. Annis, N. A. Bahcall, J. A. Bakken, R. Barkhouser, S. Bastian, E. Berman, W. N. Boroski, S. Bracker, C. Briegel, J. W. Briggs, J. Brinkmann, R. Brunner, S. Burles, L. Carey, M. A. Carr, F. J. Castander, B. Chen, P. L. Colestock, A. J. Connolly, J. H. Crocker, I. Csabai, P. C. Czarapata, J. E. Davis, M. Doi, T. Dombeck, D. Eisenstein, N. Ellman, B. R. Elms, M. L. Evans, X. Fan, G. R. Federwitz, L. Fiscelli, S. Friedman, J. A. Frieman, M. Fukugita, B. Gillespie, J. E. Gunn, V. K. Gurbani, E. de Haas, M. Haldeman, F. H. Harris, J. Hayes, T. M. Heckman, G. S. Hennessy, R. B. Hindsley, S. Holm, D. J. Holmgren, C.-h. Huang, C. Hull, D. Husby, S.-I. Ichikawa, T. Ichikawa, Ž. Ivezić, S. Kent, R. S. J. Kim, E. Kinney, M. Klaene, A. N. Kleinman, S. Kleinman, G. R. Knapp, J. Korienek, R. G. Kron, P. Z. Kunszt, D. Q. Lamb, B. Lee, R. F. Leger, S. Limmongkol, C. Lindenmeyer, D. C. Long, C. Loomis, J. Loveday, R. Lucinio, R. H. Lupton, B. MacKinnon, E. J. Mannery, P. M. Mantsch, B. Margon, P. McGehee, T. A. McKay, A. Meiksin, A. Merelli, D. G. Monet, J. A. Munn, V. K. Narayanan, T. Nash, E. Neilsen, R. Neswold, H. J. Newberg, R. C. Nichol, T. Nicinski, M. Nonino, N. Okada, S. Okamura, J. P. Ostriker, R. Owen, A. G. Pauls, J. Peoples, R. L. Peterson, D. Petravick, J. R. Pier, A. Pope, R. Pordes, A. Prosapio, R. Rechenmacher, T. R. Quinn, G. T. Richards, M. W. Richmond, C. H. Rivetta, C. M. Rockosi, K. Ruthmansdorfer, D. Sandford, D. J. Schlegel, D. P. Schneider, M. Sekiguchi, G. Sergey, K. Shimasaku, W. A. Siegmund, S. Smee, J. A. Smith, S. Snedden, R. Stone, C. Stoughton, M. A. Strauss, C. Stubbs, M. SubbaRao, A. S. Szalay, I. Szapudi, G. P. Szokoly, A. R. Thakar, C. Tremonti, D. L. Tucker, A. Uomoto, D. Vanden Berk, M. S. Vogeley, P. Waddell, S.-i. Wang, M. Watanabe, D. H. Weinberg, B. Yanny, N. Yasuda, and SDSS Collaboration. The Sloan Digital Sky Survey: Technical Summary. *AJ*, 120:1579–1587, September 2000.
- [42] Y. Zhang, P. Anninos, and M. L. Norman. Spectrum Analysis of Lyman Alpha Forest Lines from Hydrodynamical Simulations. In *American Astronomical Society Meeting Abstracts*, volume 27 of *Bulletin of the American Astronomical Society*, page 1412, December 1995.